

METHODOLOGY FOR AEROACOUSTIC NOISE ANALYSIS OF 3-BLADED H-DARRIEUS WIND TURBINE

by

**Mirko R. DINULOVIĆ^{a,*}, Marta R. TRNINIĆ^b, Boško P. RAŠUO^a,
and Dejan V. KOŽOVIĆ^c**

^a Faculty of Mechanical Engineering, University of Belgrade, Belgrade, Serbia

^b Academy of Applied Technical Studies, Belgrade, Serbia

^c Ben Air, Belgrade, Serbia

Original scientific paper

<https://doi.org/10.2298/TSCI2301061D>

The present paper presents the aeroacoustic calculation methodology for the H-Darrieus wind turbine. The CFD analysis, for different wind turbine blades' angles of attack, coupled with the noise analysis, based on Lighthill and Prudmann models is performed. This type of turbine is of particular interest since it is insensitive to wind direction and can be used in urban areas. In this study commercial software, ANSYS is used for CFD and aeroacoustic analysis. The required turbulent flow field is calculated based on the standard k-ε model, and required model constants are obtained experimentally in a low-Mach number wind tunnel. The noise levels generated by operating turbine are calculated based on Lighthill and Proudman's aeroacoustic theories. It was found that the methodology presented can be efficiently used in noise analysis of vertical axes wind turbines and due to recent strict noise regulations has to be deployed at the early design stages.

Key words: vertical-axis wind turbines, aeroacoustic model, noise

Introduction

Wind energy (often referred to as wind power) represents a renewable, sustainable, and most of all clean energy source. In recent years, worldwide, the demand for renewable energy attracted extensive attention. Apart from wind energy, mainstream technologies also considered renewable are hydropower, solar, bioenergy, and geothermal energies. However, when wind energy is considered, it is estimated that the global electric power generation capacity is over 825 GW [1]. In the period between 2012 and 2021, the electric power generation annual growth rate was estimated to be close to 13% [1]. These figures undoubtedly suggest that many countries are using (to a certain extent) wind power as an additional energy source and more importantly investing in wind-power systems expansion. Analyzing wind installed power capacity in countries that use wind energy the most is China (114 763 MW in 2014 and 328 973 MW in 2021, per renewable energy statistics, report 2022) [2]. In 2021 USA produced 132 738 MW, and the EU 187 497 MW [2].

Nowadays, systems known as wind turbines are used to transform wind power into mechanical power or electricity. These systems are in constant development, from an engineering point of view to produce electricity at the most efficient, reliable, and effective oper-

* Corresponding author, e-mail: mdinulovic@mas.bg.ac.rs

ating cost. The design, operation, and maintenance of wind turbines are very well established. In the design phase of any type of wind turbine aerodynamics, structural engineering, and fluid mechanics play an important role. Modern wind turbines can be positioned on land as well offshore in vast water areas. These modern turbines in general can be classified into two major types: horizontal-axis and vertical-axis turbines. Each of these types has its advantages and disadvantages and are both used. Horizontal turbines are similar to windmills, whereas vertical turbines are omnidirectional and independent of wind direction. Apart from this distinction, wind turbines can be divided based on their size. Based on their size (and therefore power generating capacity) wind turbines can be classified into three categories. First represent, single, small turbines capable of producing up to 100 kW which are often satisfactory for residential use, and to a certain extent moderate industrial and commercial demands. The second group is somewhat larger or utility-scale turbines that range from 100 kW to a few [mW]. These types of turbines are in general used to power electrical grids (complete or partial). Often, they are assembled into groups of turbines at the same location called wind farms or wind parks. The largest wind turbines are offshore wind turbines. According to Global Wind Report [3] 2021, as of 2020, the total worldwide offshore wind power capacity was close to 36 GW.

The essential principle in electricity generation using wind turbines is that the air-flow can be used. Modern wind turbines can operate (start generating electricity) in air-flows from as low as 2 m/s up to cut-off speeds of 25 m/s. This is important to emphasize since many regions in the world satisfy this condition and hence are candidates for the installation

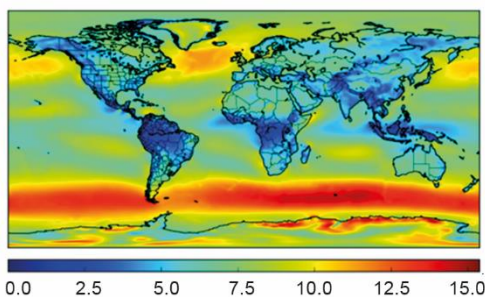


Figure 1. Mean wind speed [ms^{-1}] worldwide at 100 m

of wind turbines of various capacities and electricity generation. Figure 1 illustrates the mean wind speed worldwide at 100 m in [ms^{-1}] [4].

When vertical axis turbines are considered, their advantages render these types of turbines potential candidates for industrial and domestic use. The main advantage of this type of turbine is that there is no need for orientation of the blades since it is omnidirectional, can be designed in a variety of sizes, and can operate at relatively low wind speeds. However, the efficiency of these systems is relatively low and the self-starting procedures can cause operational problems. That is why these aspects put

these systems under constant development. Another problem (with all types of turbines, not only vertical axis turbines) is the aeroacoustic noise, that develops during the operation of the turbine. The noise can be regarded as an unwanted sound when in contrast, the sound is one of the fundamental parts of human life (used for social interaction, communication, education, and many other aspects of human life). Unwanted sound (noise) has to be eliminated from the human environment, especially in habitats with operating machinery. The importance of noise understanding, reduction, and potential elimination has drawn a lot of attention in recent years from many researchers and design engineers in recent years. On the other hand, to certify any type of mechanical system many new strict regulations and standards related to noise emission have emerged. To satisfy these conditions, the noise radiation and emission effects of operating machinery have to be considered even in the early stages of system development and design. As an example, recommendations given by The National Institute for Occupational Safety and Health (NIOSH) worker exposure to noise should be kept below a level equivalent

to 85 dB(A) for eight hours to minimize the possibility of worker's noise-induced hearing loss [5]. In the same realm as European Directive 2003/10/ EC noise exposure limits are defined. According to this directive, the exposure to noise at the workplaces, expressed as the time-weighted average of the noise exposure (for a nominal eight-hour working day) is 87 dB(A), 85 dB(A), and 80 dB(A), respectively [6]. These requirements are very strict and require great attention from the wind turbine design point of view.

In the present work, recognizing the great potential of the vertical axis turbines, the methodology of predicting the noise emissions from these systems, arising from air-flow is presented. The vertical axis turbine, of the H-Darrieus turbine with three blades, is analyzed for noise emission, and the complete methodology for the tonal and broadband noise is presented. In general, tonal noise arises from the periodic flow unsteadiness whereas broadband noise is mostly due to the interaction between the structure and the air-flow. The typical vertical axis wind turbine of the H-Darrieus type, analyzed for noise emissions in this work is presented in fig. 2.

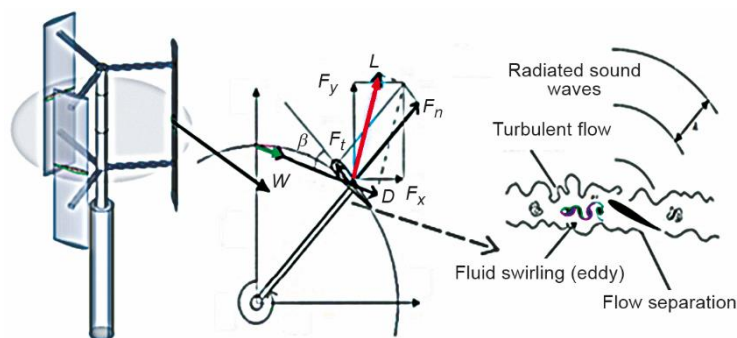


Figure 2. The 3-blade H-Darrieus wind turbine

The principle of operation of this type of turbine is as follows. When the turbine blades are exposed to the air-flow, turbine blades turn about a rotor spinning a generator. This mechanism can be derived either directly or using a shaft coupled to a series of gears. Gears can speed up the rotation from the blades allowing a smaller generator to be used. Power is created utilizing this process. The force diagram on one turbine blade, the lift force (lift force, L), and the generation of radiated sound waves are presented in fig. 2.

In the present work, sound radiation and noise generation that arises from the rotating turbine blades are calculated based on available numerical models. The broadband noise field is obtained based on the known Lighthill's acoustic analogy, obtaining the general solution to the wave equation. For the far-field, tonal noise acoustic field prediction is obtained based on Ffowcs Williams and Hawking's theory, and under the assumption that the medium is at rest at the domain infinity. The turbulent flow is simulated using the $k-\epsilon$ model, with adjusted parameters for required Reynolds numbers and blade airfoil geometries obtained experimentally using wind tunnel testing.

Aeroacoustic models

Over a surface, the hemispherical sound propagation model, which includes air absorption can be presented by [7]:

$$L_p = L_w - 20 \log_{10} r - \alpha r \quad (1)$$

where L_p [dB] is the sound pressure level at the distance r from the source with a sound power level L_w [dB]. For low Mach number flows, absorption factor, α , can be set, for most conditions, to 0.005 dBm^{-1} .

In most cases, there are no distinct tones when noise is analyzed from the acoustics point. This applies to all types of turbulent flows. The sound energy is distributed over a broad range of frequencies. For Lighthill's [8] acoustic analogy statistical turbulence quantities computed from CFD equations can be used.

For the low Mach numbers flows, noise caused by the interaction of the fluid (air, if wind turbines are in question) and the airfoil turbine blades is governed by mass conservation and Navier-Stokes momentum equations:

$$\begin{aligned}\frac{\partial \rho}{\partial t} + \frac{\partial}{\partial x_i}(\rho u_i) &= 0 \\ \frac{\partial}{\partial t}(\rho u_i) + \frac{\partial}{\partial x_i}(\rho u_i u_j + p_{ij}) &= 0\end{aligned}\quad (2)$$

In eq. (2) velocity components are denoted as u_i , u_j is the velocity and p_{ij} is the stress tensor. Further, it is convenient to express the stress tensor p_{ij} , in terms of static pressure and viscosity stress. The stress tensor is:

$$p_{ij} = -\sigma_{ij} + \delta_{ij} p \quad (3)$$

Static pressure is denoted with p , the Kronecker delta with δ_{ij} and σ_{ij} is viscosity stress. Viscosity stress is:

$$\sigma_{ij} = \mu \left[\frac{\partial u_i}{\partial x_j} + \frac{\partial u_j}{\partial x_i} - \frac{2}{3} \left(\frac{\partial u_j}{\partial x_j} \right) \delta_{ij} \right] \quad (4)$$

Mass and momentum conservation equations are used to derive equations of sound propagation and are:

$$\begin{aligned}\frac{\partial^2 \rho}{\partial t^2} - a_0^2 \nabla^2 \rho &= \frac{\partial^2}{\partial x_i \partial x_j} T_{ij} \\ T_{ij} &= \rho u_i u_j + p_{ij} - a_0^2 \rho \sigma_{ij}\end{aligned}\quad (5)$$

At the speed of sound a_0 these equations define a propagating wave in a resting medium. Externally applied (fluctuating) forces are given by the right-hand side of eq. (5). Sound propagation equation is solved by Lighthill [8] and Curle [9]. The solution is:

$$\begin{aligned}\rho'(x, t) = \rho(x, t) - \rho_0 &= \frac{1}{4\pi a_0^2} \frac{\partial^2}{\partial x_i \partial x_j} \int_V \frac{T_{ij} \left(y, t - \frac{R}{a_0} \right)}{R} dV(y) + \\ &+ \frac{1}{4\pi a_0^2} \frac{\partial^2}{\partial x_i} \int_S \frac{l_{ij} p_{ij} \left(y, t - \frac{R}{a_0} \right)}{R} dS(y)\end{aligned}\quad (6)$$

The location of interest is located at a position in the domain given with co-ordinates x and y , and is usually referred to as the acoustic observation point in eq. (6), $R(x, y)$ is the distance between acoustic observation points and the point where the sound is generated.

This approach based on Lighthill's acoustic analogy applies to the analysis of energy generated from subsonic flows. Based on Proudman's analogy, the flow-induced acoustic intensity can be expressed in terms of standard steady-state variables corresponding to the turbulent kinetic energy, k , and dissipation rate, ε . This is conventionally used in CFD analysis. Based on Lighthill's acoustic analogy Proudman [10], derived a formula for acoustic power generated by iso-tropic turbulence, however without mean flow. Due to the unit volume of isotropic turbulence acoustic power is:

$$p_A = \alpha_\varepsilon \rho_0 \left(\frac{u^3}{l} \right) \left(\frac{u^5}{a_0^5} \right) \quad (7)$$

Turbulence velocity is denoted with u and l is turbulence length in eq. 7. Speed of sound is a_0 and α_ε is a model constant expressed as a function of k and ε . Hence, the previous equation can be rewritten:

$$p_A = \alpha_\varepsilon \rho_0 \varepsilon M_t^5$$

$$M_t = \frac{\sqrt{2k}}{a_0} \quad (8)$$

Based on the calibration values given in [10] for the numerical simulations of iso-tropic turbulence the constant α_ε is initially set to 0.1.

The sound power level per volume is:

$$L_w = 10 \log \left(\frac{p_A}{p_{\text{ref}}} \right) \quad [\text{dB}] \quad (9)$$

The p_{ref} is the reference value and is set to $p_{\text{ref}} = 10^{-12} \text{ W/m}^3$ [11].

For a given turbulence field, Proudman's formula can be regarded as an approximate value of the local contribution to total acoustic power per unit volume.

Required model parameters for the surface acoustic sources in the proposed $k-\varepsilon$ turbulent model, calibration studies are performed using a low Mach wind tunnel. The wind tunnel tests (working section) are depicted in the picture, fig. 3.

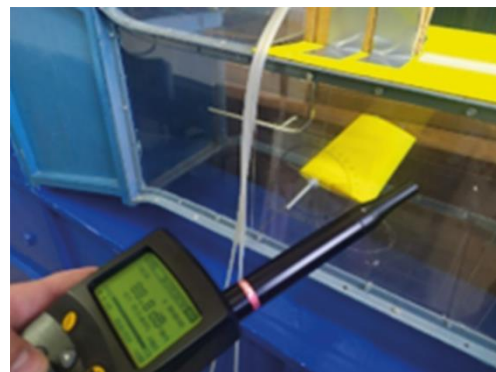


Figure 3. Airfoil noise measurement in the subsonic wind tunnel

Calibration tests were necessary to obtain $k-\varepsilon$ turbulent model constants presented in tab. 1, and are performed at inlet velocities of 5 m/s,

10 m/s, and 15 m/s. In this analysis, the standard $k-\varepsilon$ model is used proposed by Launder and Spalding [11], and is semi-empirical. It is based on the model transport equations for the turbulence kinetic energy, k , and the dissipation rate, ε . Required constants in the $k-\varepsilon$ model are determined from the experiments, with air or water as a fluid. Turbulent model constants (C_μ ,

$C_{1\varepsilon}$, $C_{2\varepsilon}$, σ_k , and σ_ε) used in this work are given in tab. 1 and the values of the constants are very close to the ones proposed by Launder and Spalding [11].

Table 1. The k - ε model constants

| C_μ | $C_{1\varepsilon}$ | $C_{2\varepsilon}$ | σ_k | σ_ε |
|---------|--------------------|--------------------|------------|----------------------|
| 0.09 | 1.42 | 1.90 | 1.00 | 1.30 |

The FW-H equations [12] can be considered the main form of Lighthill's acoustic theory developed by Lighthill [8]. The FW-H method is suitable for the computation of aerodynamic noise radiated from the structures in rotary motion [12-15]. For H-Darrieus VAWT the FW-H equations are time-domain integral formulations. These equations are suitable for computing sound pressure levels at predefined locations (receivers) generated by an operating (rotating) H-Darrieus VAWT. Pressure levels and the acoustic signals are later transformed into a frequency domain using fast Fourier transform using different known transformation algorithms:

$$\frac{1}{a_0^2} \frac{\partial^2 p'}{\partial t^2} - \nabla^2 p' = \frac{\partial^2}{\partial x_i \partial x_j} \{T_{ij} H(f)\} - \frac{\partial}{\partial x_i} \{[P_{ij} n_j + \rho u_i (u_n - v_n)] \delta(f)\} + \frac{\partial}{\partial t} \{[\rho_0 v_n + \rho (u_n - v_n)] \delta(f)\} \quad (10)$$

where u_n and v_n are velocity components normal to the surface, u_i – the fluid velocity in the x_i direction, v_i – the surface velocity in the same direction, p' – the sound pressure given as the difference $p - p_0$, and $\delta(f)$ – the Dirac's delta function.

The CFD methodology, simulation, analysis, and results

The solution to the aeroacoustic equations, and hence the noise level prediction (broadband and tonal), requires a numerical approach using computational fluid mechanics methods. Computer model of the vertical-axis wind turbine [16, 17].

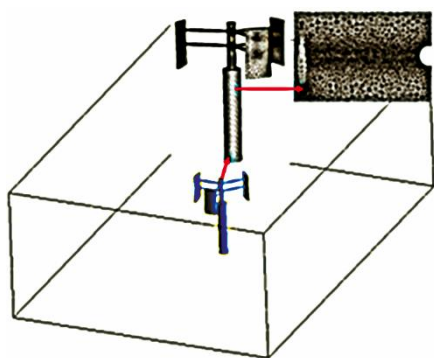


Figure 4. Computational domain for broadband noise calculations

For the broadband analysis, the complete 3-D flow field is modeled. The computational domain is discretized and presented in fig. 4.

The flow field is obtained using a k - ε turbulent model with adjusted parameters and the wave equation is solved using Lighthill's theory. Based on this approach, the most influential zones of the in-noise generation are identified which enabled further tonal analysis based on the Ffawks approach. The Broadband tonal analysis results are presented in fig. 5, and it can be seen that the wind turbine blades leading edge, trailing edge, and supports contribute the most to the overall noise levels. This brings us to the conclusion that apart from aerodynamic characteristics, which are of paramount importance in the generation of lift force, the blade airfoil characteristics, influence the overall tonal (and hence noise levels) of an operating vertical axis wind turbine [18, 19]. This conclusion, obtained in this part of the analysis suggests that this must be considered

even in the early stages of the design. For the particular case, of the wind turbine analyzed in this work, the noise levels (broadband) are in the vicinity of 60 dB, even for moderate flow velocities, which increase with blade rotation speeds, fig. 5.

The next stage, in the methodology of noise prediction, is to predict the tonal noise for the prescribed position of the receivers within the domain of interest. For this type of analysis, the known Ffwaks theory is used. The domain analyzed is presented in the following pictures, and represents the fluctuating pressure fields, during one cycle of wind turbine rotation, for azimuth rotation angles of 0°, 45°, and 90° of the leading wind turbine profile. The position of analyzed receivers is also presented at the domain location of interest. Three receivers (microphones) were positioned, aft, in the flow field at a distance of 0.5 m from the rotation zone. Once, the flow field was calculated the tonal response at the position of the receivers is calculated [20, 21]. Initially, the response of pressure *vs.* time (pressure fluctuations) is obtained, and by performing the fast Fourier transformation, based on the Hanning algorithm, the frequency response is obtained. These results are presented for different airfoil azimuth angles in figs. 6-8.

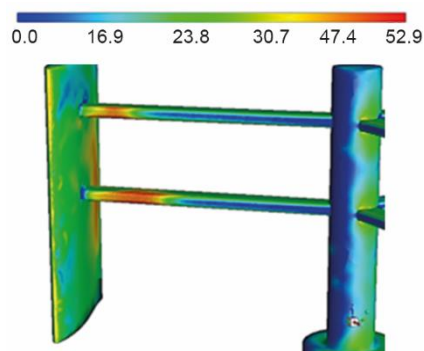


Figure 5. Broadband noise levels [dB], VAWT inlet velocity 10 m/s

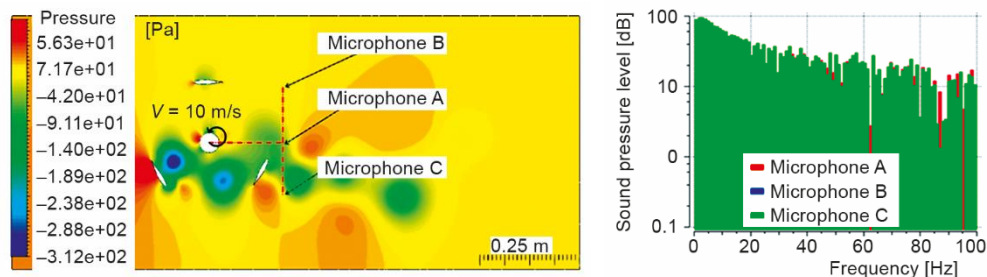


Figure 6. Pressure field and sound pressure level for azimuth angle 0° and sensor locations

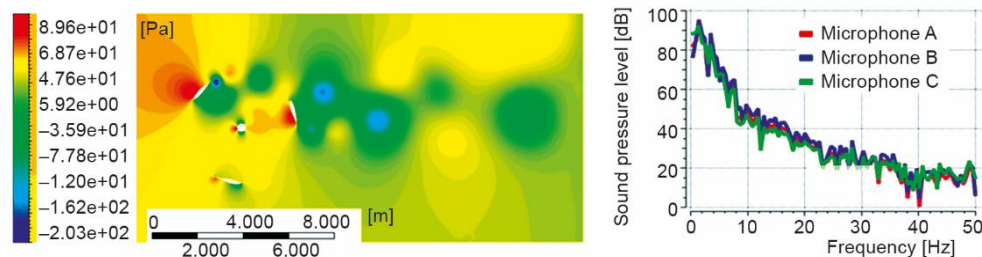


Figure 7. Pressure field and sound pressure level for azimuth angle 45°

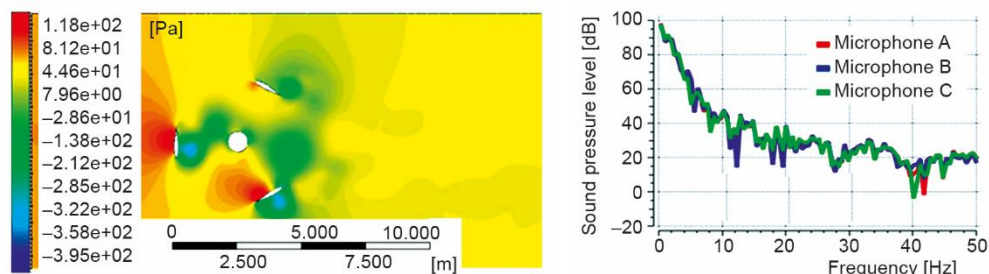


Figure 8. Pressure field and sound pressure level for azimuth angle 90°

Conclusions

In order to reduce noise levels produced during turbine operation, the aeroacoustic analysis must be performed, even at the earliest phases of design. Today, a lot of small vertical-axis wind turbines, like the H-Darrieus, are being developed, produced, and used, especially in urban areas where they can be located near people, their homes, and workplaces. There is no doubt that noise will be produced while wind turbines are in operation. It is important to reduce, if not completely eliminate, long-term exposure to noise because it can cause a variety of health issues. There are two main sources of noise in operating wind turbines. These are mechanical noise and aerodynamic noise. It was found that the aerodynamic noise, especially the noise that arises from the blade trailing edge turbulent boundary layer contributes significantly to the overall noise levels generated, and if the turbine mode of operation is performed at relatively high angles of attack, the noise that arises from the flow separation can contribute the most to the overall noise levels. If the feedback loop between trailing edge vertices and instability waves in the boundary layers is formed, noise arising from these flow conditions generates a significant amount of noise.

Based on Lighthill theory broadband noise for a rotating vertical axis turbine (Darrieus type) is estimated. Furthermore, the computational methods for the estimation of tonal noise, based on the Ffawks algorithm are also presented.

Based on analysis and calculations performed, it can be concluded, that existing aeroacoustic models can be used for noise prediction of operating turbines, both, tonal and broadband. However, the present methodology is tedious and time-consuming. Requires experimental data, which is not always at disposition to the analyst. More efforts have to be made to make the process of noise prediction more efficient.

References

- [1] ***, IRENA: World's renewable electricity capacity: <https://balkangreenenergynews.com/irena-worlds-renewable-electricity-capacity-surpassed-3-tw-in-2021/>
- [2] ***, The International Renewable Energy Agency, Renewable Capacity Statistics 2022, <https://neec.no/about/about-neec/>
- [3] ***, Global Wind Council, Global Wind Report 2021, <https://gwec.net/wp-content/uploads/2021/03/GWEC-Global-Wind-Report-2021.pdf>
- [4] Dupont, E., *et al.*, Global Available Wind Energy with Physical and Energy Return on Investment Constraints, *Applied Energy*, 209 (2018), Jan., pp. 322-338
- [5] ***, Occupational Noise Exposure, <https://www.osha.gov/noise>

- [6] ***, Directive 2003 of the European Parliament and of the Council on the Minimum Health and Safety Requirements Regarding the Exposure of Workers to the Risks Arising from Physical Agents, <https://eur-lex.europa.eu/LexUriServ/LexUriServ.do?uri=OJ:L:2003:042:0038:0044:EN:PDF>
- [7] Mollerstrom, E., *et al.*, Noise Propagation from a Vertical Axis Wind Turbine, *Proceedings*, 43rd International Congress on Noise Control Engineering, Melbourne, Australia, 2014
- [8] Lighthill, M. J., On Sound Generated Aerodynamically I. General Theory, *Proceedings of the Royal Society A*, 211(1952), 1107, pp. 564-587
- [9] Curie, N., The Influence of Solid Boundaries Upon Aerodynamic sound, *Proceedings of the Royal Society A*, 231 (1955), 1187, pp. 505-514
- [10] Sarkar, S., Hussaini, M. Y., Computation of the Sound Generated by Isotropic Turbulence, NASA Contractor Report No: 93-74, 1993
- [11] ***, ANSYS FLUENT 12.0, Theory Guide – 14.2.2 Broadband Noise Source Models
- [12] Yue, Q., Aerodynamic Noise Prediction and Reduction of H-Darrieus Vertical Axis Wind Turbine, *Australian Journal of Mechanical Engineering*, On-line first, <https://doi.org/10.1080/14484846.2021.1950359>, 2021
- [13] di Francescantonio, P. A., New Boundary Integral Formulation for the Prediction of Sound Radiation, *Journal of Sound and Vibration*, 202 (1997), 2, pp. 491-509
- [14] Peric, B., *et al.*, Comparative analysis of numerical Computational Techniques for determination of the Wind Turbine Aerodynamic Performances, *Thermal Science*, 25 (2021), 4A, pp. 2503-2515
- [15] Qiu, L., *et al.*, Airfoil Profile Optimization of an Air Suction Equipment with an Air Duct, *Thermal Science*, 19 (2015), 4, pp. 1217-1222
- [16] Kavade, R. K., *et al.*, Performance Analysis of Small-Scale Variable Pitch Vertical Axis Wind Turbine, *FME Transactions*, 50 (2022), 2, pp. 322-330
- [17] Ismaeel, T. A., *et al.*, Energy Recovery of Moving Vehicles' Wakes in Highways by Vertical Axis Wind Turbines, *FME Transactions*, 48 (2020), 3, pp. 557-565
- [18] Biadgo, A. M., *et al.*, Numerical and Analytical Investigation of Vertical Axis Wind Turbine, *FME Transactions*, 41 (2013), 1, pp. 49-58
- [19] Svorcan, J., *et al.*, Multi-Objective Constrained Optimizations of VAWT Composite Blades Based on FEM and PSO, *FME Transactions*, 47 (2019), 4, pp. 887-893
- [20] Yigit, C., *et al.*, Effect of Two-Dimensional Profile Optimization on Vertical Axis Wind Turbine Power Performance, *Tehnicki vjesnik-Technical Gazette*, 28 (2021), 1, pp. 256-263
- [21] Rašuo, B., *et al.*, A Study of Aerodynamic Noise in Air Duct Systems with Turning Vanes, *FME Transactions*, 49 (2021), 2, pp. 308-314